(54) Title: COMPUTER AIDED TREATMENT PLANNING AND VISUALIZATION WITH IMAGE REGISTRATION AND FUSION

(57) Abstract: A computer based system and method of visualizing a region using multiple image data sets is provided. The method includes acquiring first volumetric image data of a region and acquiring at least second volumetric image data of the region. The first image data is generally selected such that the structural features of the region are readily visualized. At least one control point is determined in the region using an identifiable structural characteristic discernable in the first volumetric image data. The at least one control point is also located in the at least second image data of the region such that the first image data and the at least second image data can be registered to one another using the at least one control point. Once the image data sets are registered, the registered first image data and at least second image data can be fused into a common display data set. The multiple image data sets have different and complimentary information to differentiate the structures and the functions in the region such that image segmentation algorithms and user interactive editing tools can be applied to obtain 3d spatial relations of the components in the region. Methods to correct spatial inhomogeneity in MR image data is also provided.

COMPUTER AIDED TREATMENT PLANNING AND VISUALIZATION
WITH IMAGE REGISTRATION AND FUSION

SPECIFICATION

FIELD OF THE INVENTION

5   The present invention relates generally to surgical planning and more particularly relates to systems and methods of registering, segmenting and analyzing image data for three dimensional interactive computer visualization and surgical planning and follow-up evaluation.

BACKGROUND OF THE INVENTION

10   In many areas of medical treatment, it would be beneficial for a medical practitioner to be able to visualize a region for which treatment is contemplated and to accurately simulate the contemplated treatment. By visualizing the effect of the simulated treatment and altering the proposed treatment to optimize the results in a virtual setting, results can be improved and risks associated with the

15   actual treatment can be reduced. This is particularly true in the case of invasive procedures such as surgery, biopsies and prosthesis implantation. The virtual setting would serve both as a tool for the guidance for actual treatment and as a "gold standard" for evaluation of the actual treatment and for follow-up management. Such a system can also provide an intuitive tool for medical training.

20   Preoperative imaging, such as by computerized tomography (CT), magnetic resonance imaging (MRI), ultrasound (US) and the like, is considered an important element in surgical planning. These conventional imaging technologies provide two dimensional (2D) image slices which illustrate key anatomic structures in a region of interest. However, the 2D slice images are limited in their ability to

25   represent the spatial relationships between adjacent and interrelated structures. For example, a retro-displaced bifurcation point of carotid arteries might make stenosis analysis and plaque removal planning difficult. Three-dimensional (3D) information would be very helpful for planning surgical therapy.

Traditionally, spatial anatomical relationships could only be surmised
by mentally integrating sequential 2D slice images. However, the advent of 3D
computer graphical visualization techniques and high-resolution image scanning now
allow 3D images (either surface-based or volume-based) to be constructed from

5   sequential slice images and be displayed on a computer screen. Three-dimensional
relationships between adjacent organs can be shown by interactively manipulating
these virtual organs on the screen using a mouse or some other interactive devices.
Over the past decade, many applications of such techniques in a number of areas of
medicine, including otology, and neurology have been explored.

10   To achieve more accurate tissue classification and insight regarding
tissue functionality, a series of single modality images and multi-modality images can
be utilized. The single modality images can be of a common region acquired at
different times or different orientations. In multi-modality images, the same region is
imaged using two or more imaging technologies, such as CT, MRI and US in order to

15   take advantage of the properties of each technology since a certain modality image
may be sensitive to certain kind of tissues or their functions. By using single modality
image series and multi-modality images, more information can be obtained, and
limitations of certain modality can be mitigated.

          The use of multiple image sets (including multi-modality images and

20   or single modality image series) would be useful to perform virtual visualization and
treatment planning for carotid artery stenosis and other conditions. Carotid artery
stenosis is the most common cause of stroke, which is a major health care problem,
that affects more than 700,000 Americans each year. In fact, this condition is the
leading cause of disability and the third leading cause of deaths in the United States,

25   after cardiovascular disease and cancer. Stenosis arises from the formation of plaque
(consisting of calcification. cholesterol, and blood elements). The surgical procedure
to remove plaque from a neck artery is called carotid endarterectomy. Prior to
endarterectomy, the degree of stenosis needs to be measured and the position of the
plaque must be localized. Currently available methods for evaluating carotid stenosis

30   include, for example, carotid Doppler ultrasound and contrast angiography, which
have been demonstrated for accurate determination of the degree of luminal stenosis.

2

However, luminal narrowing is an indirect marker of plaque size and may
underestimate the plaque burden as plaque may grow inside the vessel wall from the
lumen towards the outer surrounding tissues. It is desirable that plaque size (both
inwards and outwards boundary) and composition are accurately measured. These
5   measures are of value since both plaque rupture and plaque removal carry risk. The
measures relating to plaque composition and the likelihood of rupture can offer
valuable risk assessment for the decision whether or not to proceed with a plaque
removal operation.

Currently, MR data, CT data and US data each provide some insight
10   into the structure, nature and position of stenosis within an artery. However, neither
imaging technology alone is sufficient to provide a complete analysis of the size,
composition and position of the plaque buildup. The benefits of these imaging
technologies are largely complimentary and there would be a great benefit in having
the ability to readily register images of a region using these complimentary
15   technologies and to fuse the images into a single display. There is also a benefit in
having the ability to register and fuse a series of single mode images to capture
complimentary information contained therein.

In MR image data, the inter-slice and even intra slice image data often
contains spatial inhomogeneity which adversely affects automated analysis of these
20   images. Correction for spatial intensity inhomogeneities in inter- and intra- slices
provides improved results in automated quantitative analysis of MR images. The
inhomogeneities locally alter image intensity mean, median, and variance. It is
known that they vary over time and with different acquisition parameters and
subjects. For virtual treatment planning, a general purpose correction algorithm that
25   can work for any scanning protocol and anatomy region is desirable. The concept of
correcting image artifacts can be applied to the beam-hardening problem encountered
in CT images as well as the attenuation distortion in US images.

Accordingly, there remains a need for improved medical treatment
planning tools for optimizing the procedures and for evaluating the results.
30

SUMMARY OF THE INVENTION

It is an object of the present invention to provide a method of flexible image registration suitable for use in three dimensional (3D) visualization systems.

It is a further object of the present invention to provide a method of

5   visualizing a region using multiple image sets, such as a set of single-modality images or multi-modality images, in a manner where complimentary image data properties can be fused in a common, registered display.

In accordance with one embodiment of the present method, a computer based method of visualizing a region using multiple image data sets is provided. The

10   method includes acquiring first volumetric image data of a region and acquiring at least second volumetric image data of the region. The first image data is generally selected such that the structural features of the region are readily visualized. At least one control point is determined in the region using an identifiable structural characteristic discernable in the first volumetric image data. The at least one control

15   point is also located in the at least second image data of the region such that the first image data and the at least second image data can be registered to one another using the at least one control point. Once the image data sets are registered, the registered first image data and at least second image data can be fused into a common display data set.

20   The method can be used in connection with the visualization of branched structures, such as arterial structures. In this case, a bifurcation point in the arterial structure can be selected as the control point .

The first image data and the additional sets of image data can be of the same region at different times, of the same region with different patient orientations,

25   or of the same region using different imaging modes. The various sets of images, either single-modality image sets or multi-modality images, are selected to provide complimentary imaging characteristics. For example, in the case of visualizing an arterial structure for carotid stenosis, a first imaging mode can be used to delineate the arterial lumen, a second imaging mode can be used to delineate fatty components of

30   plaque deposits and third imaging mode can be used to delineate calcification components of plaque deposits.

A method is also provided for correcting spatial inhomogenieties
which may occur in MR image data. After acquiring the MR image data, a bias field
associated with the image data is estimated. The bias field is then applied to the MRI
data to correct for the spatial inhomogenieties.

5   A method is also provided to assist a user, such as a physician, in
editing the computer-aided, automatically processed results of a visualization, such as
the segmentation of the tissues within the region from the multiple image sets. The
user employs a graphical user interface to introduce editing to the multiple image sets.
Such editing can also be used to manually optimize the registration and fusion
10   operations for the multiple image sets.

BRIEF DESCRIPTION OF THE DRAWING

Further objects, features and advantages of the invention will become
apparent from the following detailed description taken in conjunction with the
accompanying figures showing illustrative embodiments of the invention, in which:

15   Figure 1 is a simplified flow diagram illustrating an overview of a
method for computer aided treatment planning and interactive visualization;

Figure 2 is a simplified block diagram of a system suitable for
performing the present method of computer aided treatment planning and interactive
visualization;

20   Figure 3 is a flow diagram illustrating an overview of a flexible
registration process for aligning multiple sets of image data, such as in multi-modality
imaging and single-modality image series acquisition;

Figure 4 is a pictorial diagram illustrating a section of a blood vessel
with plaque build up resulting in stenosis;

25   Figure 5 is a pictorial diagram illustrating a branched section of a
blood vessel with plaque build up resulting in stenosis, the branched section featuring
a bifurcation point which can be used as a control point for image data registration;

Figure 6 is a pictorial diagram of a branched section of a blood vessel
further illustrating the location of the bifurcation point which can be used as a control
30   point for image data registration;

Figure 7A further illustrates the determination of the control point for a spherical model;

Figure 7B illustrates the application of the control point and coordinate system of Figure 7A as applied to a deformable model.

5   Figure 8 is a flow diagram further illustrating the method of Figure 3 as applied to a method of visualizing and analyzing carotid stenosis.

Figure 9 is a flow diagram illustrating a process for correcting spatial inhomogenieties in MRI image data.

Figure 10 is a pictorial diagram illustrating an exemplary graphical

10   user interface display illustrating segmented multi-modality images after a fusion operation.

Throughout the figures, the same reference numerals and characters, unless otherwise stated, are used to denote like features, elements, components or portions of the illustrated embodiments. Moreover, while the subject invention will

15   now be described in detail with reference to the figures, it is done so in connection with the illustrative embodiments. It is intended that changes and modifications can be made to the described embodiments without departing from the true scope and spirit of the subject invention as defined by the appended claims.

DETAILED DESCRIPTION OF PREFERRED EMBODIMENTS

20   Figure 1 is a flow chart which illustrates an overview of the present method of computer aided treatment planning and interactive visualization which is generally performed on a computer based system, such as that illustrated in Figure 2. The invention will be described in terms of medical applications performed on human patients and in the context of medical treatment, such as examination (e.g.,

25   measuring carotid stenosis and quantifying plaque components), surgery (e.g., removal of carotid plaque), prosthesis implantation, biopsy, medication, therapeutic radiation, therapeutic ultrasound and the like. It will be appreciated, however, that the invention is not limited to human patients, nor to the exemplary list of treatments referenced. The term treatment is used to mean an intervention in a region, such as

30   but not limited to tissue, that is intended to effect an alteration of the region.

Referring to Figure 1, the method includes the initial step of generating a three dimensional (3D) image representation of a region for which some form of medical treatment or intervention is contemplated (step 102). Generating such a 3D image representation generally involves acquiring a sequential series of 2D slice

5   images, such as from a spiral computed tomography (CT) scanner, magnetic resonance imaging (MRI) scanner or ultrasound scanner (US) and transforming this 2D image data into a volumetric data set which provides a 3D representation of the region on a 2D display, such as a computer monitor. Such a technique is well known in the art, and is discussed, for example in U.S. Patent No. 5,971,767 to Kaufman et.

10   al., which is hereby incorporated by reference in its entirety.

After the 3D image is presented to a user, such as a physician, some form of virtual intervention, which simulates at least a portion of a proposed treatment, is applied to the 3D image (step 104). The virtual intervention can take on several forms, such as the quantifying of arterial stenosis and plaque components,

15   removal of tissue or artery plaques, the repair or reconstruction of a diseased or malformed organ (e.g., inner ear, lungs, liver, joints, etc.), the placement of a prosthetic implant, the placement of a stent graft, the placement of biopsy needle, the placement of therapeutic radiation and the like.

Using the resulting 3D image, and possibly the assistance of computer

20   generated models of the applied intervention, the results of the virtual intervention can be evaluated and warnings can be generated indicative of high levels of risk attendant with the proposed intervention (step 106). Based on the displayed results, and any warnings provided, the user can repeatedly modify the proposed intervention (step 108) and apply the modified intervention to the 3D image (step 104) until a

25   satisfactory result is ascertained or it is determined that the proposed treatment is not feasible. Several alternative interventions can be saved in a database to compare the risks and efficacy of proposed alternative intervention plans. The quantified arterial stenosis and plaque components will provide a measure of risk factor for plaque rupture, which can result in stroke, pulmonary embolism, and occlusions in the liver

30   and kidneys.

After the proposed intervention is finalized, the final intervention can be simulated and the results fully applied to the 3D image (step 110). The user can then view the results and navigate in and around the region to determine the efficacy of the proposed treatment (step 112). The planned results can then be used as a guide

5   for the actual treatment with coordinate registration between the virtual model and the patient and as a gold standard to evaluate the actual intervention during post-intervention follow up examinations.

Figure 2 is a simplified diagram of an exemplary system for performing the present computer aided treatment planning and interactive

10   visualization methods. In this exemplary embodiment, a patient 201 lies down on a platform 202 while scanning device 205 scans the area that contains the organ or organs which are to be examined. The scanning device 205 contains a scanning portion 203 which acquires image data of the patient and an electronics portion 206. Electronics portion 206 generally includes an interface 207, a central processing unit

15   209, a memory 211 for temporarily storing the scanning data, and a second interface 213 for sending data to the virtual navigation platform. Interface 207 and 213 can be included in a single interface component or can even be the same component. The various operational components and subsystems in electronics portion 206 are connected together with conventional connectors.

20   The data from the scanning portion 203 is generally in the form of a stack of two dimensional image slices of a region of interest, which are provided from conventional spiral CT, MRI or US scanners. Central processing unit 209 converts the scanned 2D data to a 3D voxel data representation, in a manner known in the art, and stores the results in another portion of memory 211. Alternatively, the converted

25   data can also be directly sent to interface unit 213 to be transferred to the virtual navigation terminal 216. The conversion of the 2D data could also take place at the virtual navigation terminal 216 after being transmitted from interface 213. Preferably, the converted data is transmitted over carrier 214 to the virtual navigation terminal 216 in order for an operator to perform the computer aided treatment planning. The

30   data can also be transported in other conventional ways such as storing the data on a

storage medium and physically transporting it to terminal 216 or by using satellite transmissions.

The scanned data need not be converted to its 3D representation until the visualization rendering engine requires it to be in 3D form. This may save

5   computational steps and memory storage space.

Virtual interactive visualization terminal 216 includes a screen 217 for viewing the image data, an electronics portion 215 and interface device 219 such as a keyboard, mouse or track ball. The electronics portion 215 generally includes a interface port 221, a central processing unit 223, other components 227 necessary to

10   run the terminal and a memory 225. The components in terminal 216 are connected together with conventional connectors. The converted voxel data is received in interface port 221 and stored in memory 225. The central processor unit 223 then assembles the 3D voxels into a virtual representation which can be displayed on screen 217. Preferably, a graphics accelerator which is optimized for volume

15   rendering can also be used in generating the representations. The virtual interactive visualization terminal 216 can be embodied using a high speed graphics work station, such as manufactured by Silicon Graphics, Inc., or in a high speed personal computer, such as an IBM compatible computer with a Pentium III (or higher) processor having a 1GHZ or faster clock speed.

20   The operator can use interface device 219 to interact with the system 200, such as to indicate which portion of the scanned body is desired to be explored. The interface device 219 can further be used to control the image being displayed, including the angle, size, rotation, navigational position and the like.

Scanning device 205 and terminal 216, or parts thereof, can be part of

25   the same unit. Numerous CT, MRI, and US systems are suitable for such applications. A single platform may be used to receive the scanned image data, convert the image data to 3D voxels if necessary and perform the guided navigation.

In many virtual visualization and surgical planning operations, the use and registration of multiple images is desirable. This can be the result of acquiring

30   multiple sets of image data from a region over time, acquiring multiple image sets of a region using different patient orientations, or by acquiring multiple image sets of a

9

region using various technologies to exploit the advantages of various imaging techniques. When multiple sets of image data are acquired, such image sets must by registered in some manner in order to reasonably use the data in each image set. Exact image registration, for example, a voxel specific registration process, can be

5   very difficult to achieve and is processor intense. In many applications, such precise registration is not required.

Figure 3 is a flow diagram illustrating an overview of a flexible registration process for aligning multiple sets of image data, such as in a series of single-modality images and in multi-modality imaging which can be practiced using

10   the system of Figure 2 and variations thereof. This process will be described in connection with the visualization and analysis of plaque build up within a blood vessel, but is extendible into many forms of single-modality image sets, multi-modality imaging and other multiple image set registration applications. In step 305, a first set of image data is acquired. In the case of arterial stenosis, the first set of

15   image data may be acquired using 3D time-of-flight magnetic resonance angiograpy (TOF MRA). The 3D TOF MRA has proven to be an effective imaging technique for providing good enhancement of the arterial lumen. Thus, the gross structure of the arterial lumen and the suspect location of a plaque build up can be identified using this imaging technique. However, TOF MRA does not provide optimal resolution at

20   distinguishing the characteristics among soft tissues and the components of the plaque.

In step 310, a second set of image data is acquired. As noted above, this can be image data acquired at a different time, a different patient orientation or with a different imaging technology. In the case of arterial stenosis, a second imaging

25   mode is used to provide a set of image data which can be segmented to distinguish characteristics of the soft tissue and plaque. For example, T_1-weighted MR imaging (T_1-MRI) has been found to provide good contrast and can be performed in the same MRI series as the TOF MRA. In order to obtain additional information, yet another set of image data can be acquired to provide features not easily distinguished in the

30   previous image data sets. For example, MRI data does not readily distinguish a

calcification component of the plaque. To properly determine the total volume and
composition of the plaque, a CT image dataset of the region can also be acquired.

Using one set of the image data acquired in steps 305 and 310 the
major structural characteristics of the region, including possible suspect regions, can
5   be ascertained (step 315). As noted above, the TOF MRA image data provides a good
rendering of the 3D arterial lumen and can be used to identify any regions of possible
stenosis.

Figure 4 is a pictorial diagram illustrating a section of a blood vessel
with plaque build up resulting in stenosis. The arterial lumen 400 is shown with a
10   region of plaque 405 impinging on the lumen resulting in stenosis. The lumen can be
characterized by a diameter of the normal vessel (B) 410 and a minimum diameter at
the location of the stenosis (A) 415. The degree of stenosis can be characterized by
the definition set forth by the North American Symptomatic Carotid Endarterectomy
Trial (NASCET). The NASCET is determined as :

15
$$\frac{B-A}{B} X100\%$$

Figure 5 is a pictorial diagram illustrating a branched section of a
blood vessel with plaque build up resulting in stenosis. From step 315, the lumen of
the artery 505 can be extracted and the regions of possible stenosis 505 can be
identified. In addition, a centerline skeleton of the arterial structure can also be
20   determined. In Figure 5, the artery exhibits a first arterial section 510 which branches
at a bifurcation point 515 into an internal arterial branch 520 and an external arterial
branch 525.

After at least one set of image data has been processed to determine the
structural characteristics of the region (step 315), at least one control point is
25   established using a consistently identifiable structural characteristic of the region (step
320). Referring to Figure 5, in the case of a branched arterial structure, the
bifurcation point 515 can be determined and selected as the control point for
subsequent registration operations.

Figure 6 is a pictorial diagram of a branched section of a blood vessel
30   further illustrating the location of the bifurcation point which can be used as a control

point for image data registration. From the skeletal centerline of the arterial lumen
the bifurcation point can be determined. Referring to Figure 6, the bifurcation point is
refined as being the center of a maximal diameter sphere that fits within the lumen at
the bifurcation region. Using the center of the maximal sphere as the origin, a

5   coordinate system, such as X, Y and Z axes, can be defined in the region for
subsequent registration. A number of different coordinate systems can be used. For
example, a Cartesian coordinate system can be used which corresponds to the
orientation of the human body being imaged, e.g., with the Z-axis aligned along the
height of the body (e.g., from head to toe), the Y-axis oriented from back to front and

10   the X axis running laterally (e.g., from left to right). The units of length for the
coordinate system can be arbitrarily set to one voxel or some other convenient unit of
measure. The absolute magnitude of the units used will vary based on the acquisition
properties of the imaging scanner being used.

          Figure 7A further illustrates the determination of the control point and

15   the registration between a spherical model and its deformable model. As illustrated in
Figure 7A, three mutually orthogonal planes aligned along a Cartesian coordinate
system are defined which can readily be applied to a deformable model, such as that
illustrated in Figure 7B. The two coordinate systems can be registered by aligning
them each to a reference coordinate system. The reference coordinate system can be

20   one which is associated with anatomical axes of the human body. This flexibility
allows registration of multiple image sets despite variations in resolution and other
variables.

          Returning to Figures 3 and 5, using the control point 515 and the
structural characteristics of the region, the approximate location of suspect regions is

25   determined in at least one of the sets of image data (step 325). In the case of carotid
stenosis, the location of the suspect regions is determined by finding the areas of
minimum diameter 530 in the lumen, which correspond to areas of maximum stenosis
in a region of plaque. The location of the suspect region can be determined in a
number of ways. For example, the curve length L from the control point 515 to the

30   point of minimum diameter 530 along the skeletal centerline provides a first measure
of location. In addition, the "vertical" distance H, which is measured along the

imaginary Z-axis of the coordinate system framing the control point 515, can be used to determine the relative position of the suspect region with respect to the control point.

After the control point(s) and the position of suspect areas have been
5   identified in a first image data set, registration of the first image data set with the additional image data sets can take place (step 330). The process of flexible registration entails identifying the control point(s) in each image data set and using the control points as a datum for registration of the image data sets. For example, in the example of a branched arterial structure discussed above, the bifurcation point
10   would be located in each set of image data. In the case of T_1-weighted MR images, generally the bifurcation point is manually identified by a user of the system, such as a physician. The image data sets are registered to one another using the control point(s) and are aligned to the coordinate system which is assigned. Assuming an affine model of the region being imaged, three control points can be used to fully
15   automatically register the coordinate systems of the image data sets in 3D space. With less than three control points, the registration process can be initially automated and then completed using manual intervention to optimize the registration process.

Using an appropriate transfer function, the voxels of the arterial lumen can be displayed as a translucent structure with the skeletal centerline therein. In
20   addition, the suspect regions can be highlighted on the skeletal centerline by emphasizing the suspect regions, such as by using a different color to display suspect regions.

To determine the location of stenosis, the information from the first image data set, in this case the previously processed results of TOF MRA, are
25   preferably used. The bifurcation point is detected in the T_1-weighted MR images, generally, manually by physician. The same coordinate system defined with respect to the first image data set is then applied to the T_1-weighted MR images. Starting at the control point, the vertical distance H is measured along the Z-axis to arrive at the position corresponding to the approximate location of the stenosis in the second set of
30   image data (step 335). In the T_1-weighted MR images the vessel lumen is difficult to differentiate. However, if an imaging technology is employed which offers adequate

delineation of the vessel lumen, the distance L along the center line of the lumen to
the suspect region can also be used. Exact voxel accuracy of location is not necessary
in aligning the images. The important criteria is that a suspect region in the image data
covers the entire region of stenosis and plaque which has been identified in step 325.

5   Image segmentation can then be performed in the region of plaque to
determine the nature and composition of the plaque build up (step 340). If the plaque
has fatty components, those components will exhibit a higher intensity in the T_1-
weighted MRI image as compared to both the vessel lumen and the vessel wall. Such
components can be detected and identified in the segmentation results of the T_1-

10   weighted MR images. The volume of the fatty components can be quantified and a
3D model of the plaque can be created.

As noted above, the TOF MRA data set provides good delineation of
the lumen whereas the T_1-weighted MR data provides good segmentation results for
the fatty components of the plaque causing the stenosis. By employing flexible

15   image registration and then fusing the registered datasets into a single display data set,
a single display providing the enhanced features of both the arterial structure and the
plaque can be provided (step 345).

Image fusion can take on several forms but generally results in at least
a portion of the features of each image set being presented simultaneously or at least

20   selectively on a common display and in a common registration. Generally, each set of
image data, whether multi-modality image data or a series of single-modality image
data sets, is pre-processed through an image segmentation process. Image
segmentation is used to emphasize and extract various features in the sets of image
data. One or more sets of image data can be selected to display the raw image data.

25   In the case of arterial imaging for carotid stenosis, this would generally by the TOF
MRA image data or US image data which effectively delineates the arterial lumen.
Segmented portions of the other image data sets can be simultaneously or selectively
rendered on the display. Each of the sets of image data can be rendered as a layer in
the display to effectively render the region of interest. For example, in viewing a

30   region of stenosis, an operator can selectively heighten the image data from the T_1-
weighted MR data to emphasize fatty components of the plaque or the CT image data

to emphasize the calcification components of the plaque. The rendering can be performed initially in an automated manner than optimized by the user, generally by use of a GUI interface. In addition, the operator can generally navigate in the image data, change views, zoom, etc. The processing of the present method effects these

5   navigation and manipulation commands on all fused image data sets such that all interaction is effected on all image models. This is possible because the sets of image data are registered to one or more common control points and are aligned to a common coordinate system.

The T_1-weighted MR data provides good segmentation results for the

10   fatty components of the plaque but generally can not reliably distinguish the calcification components of the plaque. Generally, CT image data exhibits higher spatial resolution and better contrast between calcification and other tissues. Thus, it is desirable to scan the region with a CT scanner to acquire CT image data which can also be flexibly registered with the TOF MRA data set.

15   In the CT image data set, the vessel lumen and wall have similar intensity values as that of soft tissue. As a result, the arterial lumen is difficult to delineate in a CT image. A first approach to overcome this issue is to perform CT image scanning twice. In a first imaging scan, CT angiography (CTA) is acquired following the injection of a contrast agent in the blood. From the CTA image data,

20   the carotid lumen will be delineated. The skeleton along the centerline of the lumen can be generated and the bifurcation point can then be determined. By tracing the skeleton up-stream the distance L, the stenosis location can be detected. The second CT imaging scan is acquired with the same scanning settings, but without the presence of the contrast agent. In the second scan, only calcification regions are

25   depicted as regions of increased intensity. Since the field of view (FOV) and scanning setting are identical, the two scans are assumed to be registered at voxel-specific accuracy. The region of stenosis in the second scan is then considered to be the same as that in the CTA scan. Then, a suitable segmentation algorithm can be applied to the region of stenosis to extract the region of calcification. The volume of

30   the calcification can be measured and a 3D model of it can be created.

The second approach to using the CT imaging data to determine the regions of calcification does not use a CTA scan with a contrast agent. Instead, the stenosis region is detected manually in the CT images. This task is generally performed by a physician with help of image rendering tool. Various forms of image rendering tools are known in the art and generally provide a graphical user interface (GUI) which allows the user to readily manipulate both the individual image slices and the 3D virtual model on a computer screen. An example of one such GUI display is depicted in Figure 10. Anatomical knowledge of the structure, such as the carotid artery, is generally used in this procedure.

Figure 10 illustrates an exemplary GUI display of a fused display of a segmented object 1005 within the raw CT image data of the region of interest 1000, in this case the bladder of a patient. In the view depicted in Figure 10, the image data is presented as a 3D body in 2D forms, i.e. the image is shown in cut away slices in two orthogonal directions and projecting in a third direction. The GUI includes on-screen controls 1010 which can be selected and modified using either a computer keyboard or digital pointer, such as a mouse, trackball and the like. Using the GUI the user can inspect details of the image, edit the segmentation results, change the view and the like.

After detecting a suspect region, such as an area of possible stenosis, the suspect region image is segmented and processed substantially as described above. While this second process requires further manual intervention, it does not require the use of a second CT scan or the use of a contrast agent.

While in the above example, TOF-MRA and CTA imaging were described as imaging methods to determine the arterial lumen, it will be appreciated that US imaging can also be used in place of one or both of these imaging techniques.

Determination of Likelihood of Rupture

The plaque which forms in the arterial lumen and results in stenosis is generally composed of blood volume, fatty components and calcification components. The total volume of the plaque can be obtained by summation of the volume of fatty components identified in the T_1-weighted MR image data whereas the calcification

components can be determined from the segmented CT image data. The percentage
of each component can be calculated. The larger the volume of blood or its
percentage, the higher the probability of a rupture of the plaque, with increased
attendant risk of stroke. In addition, a close proximity of blood deposits near the

5   surface of the plaque build up also provides an indication of high risk of rupture. The
level of risk is not quantifiable in absolute terms. However, by employing an
arbitrary scale for both blood volume and surface depth, a weighted relative risk
factor can be associated with the stenotic region. Based on such "risk scales," regions
of risk can be highlighted, such as by use of one or more different display colors, to

10   alert the user of the risk. The risk factor values can also be compared to
predetermined or user defined threshold values, which if met or exceeded, would
trigger more active alarm indications to the user.

            The volume of the blood inside the plaque and its location near the
boundary are two indicators for the likelihood of rupture. Therefore, accurate

15   segmentation of the plaque components and identification of their spatial relation are
objectives in stroke risk assessment. In the present systems and methods information
from (1) CT/CTA (calcification), (2) TOF MRA or US(lumen), and (3) T_1-weighted
MRI (fatty, blood, and others) images are simultaneously used to render this
information. The information is represented together to show the tissue spatial

20   relation in 3D space. This requires the use of both image registration and image
segmentation computer processing techniques. Each of these operations benefit from
a degree of user editing. The editing can be performed by displaying the segmented
objects inside the raw image or by displaying all segmented objects together, as
depicted in Figure 10.

25   Figure 8 is a flow chart summarizing the application of the method of
Figure 3 as specifically applied to the visualization and analysis of an arterial
structure for carotid stenosis. In step 805 image data is acquired to visualize the
arterial wall and lumen. This generally takes the form of TOF MRA or US image
data. After image segmentation, the arterial wall and lumen are clearly

30   distinguishable in the MRA or US image data (step 810). From the MRA image
which illustrates the lumen, the centerlines of the lumen are calculated and the

17

bifurcation point is located as the control point (step 815). Suspect regions are located in the lumen which may reflect areas of stenosis (step 820). The position of these suspect regions is then determined with respect to the control point and an arbitrary coordinate system which is defined around the control point.

5   In addition to the TOF MRA image data, a second set of image data is acquired to highlight fatty components within the suspect regions (step 825). Generally, a T_1-weighted MRI image data set has been found acceptable for this purpose. The control point and coordinate system which was defined in the first image data are then located and placed in the second image data set and the position

10   of the suspect regions are located (step 830). Image segmentation is performed on the second image data set in the suspect regions to highlight the fatty components of the plaque deposits.

A third image data set is acquired to delineate the calcification components of the plaque deposits (step 840). This third image data set can take the

15   form of CT image data. Within the third image data set, the control point and coordinate system are identified and placed and the position of the suspect regions are identified (step 845). Again, image segmentation in the suspect regions can then be performed to delineate the regions of calcification (step 850).

Using the control point and coordinate system which has been located

20   in each set of image data, the sets of image data are registered with one another and fused into a single display image which can be presented on the display of the visualization system (step 855). Using the fused image, the user can readily analyze the suspect regions, for example to determine the volume and composition of any plaque deposits, the likelihood of rupture and the quality of the arterial surface for

25   receiving a stent graft (step 860).

Spatial Inhomogeneity Correction

In MR image data, the inter-slice and intra-slice image data often contains spatial inhomogeneities which adversely affect automated analysis of these images. Correction for spatial intensity inhomogeneities in inter- and intra- slices

30   provides improved results in automated quantitative analysis of MR images. The

inhomogeneities locally alter image intensity mean, median, and variance. It is
known that they vary over time and with different acquisition parameters and
subjects. For virtual treatment planning, a general purpose correction algorithm that
can work for any scanning protocol and anatomy region is desirable.

5   A correction method based on known renormalization group theory has
now been found to be useful for the spatial inhomogeneity of MR image data. As
illustrated in Figure 9, following image data acquisition (step 905), the correction
method consists of two primary steps. The first step is to estimate an inhomogenous
bias field (step 910). The second step is to correct the MR image based on that bias

10   field (step 915).

The notations which will be used in connection with the present
renormalization transformation (RT) method for MR image are now presented. Let S
be a single-connected, finite subset of the 2D integer lattice. One can consider S as
the pixel locations of a region of interest (ROI) in a 2D image. Let $X = \{x_i : i \in S\}$ be an

15   image, where x_i is the intensity value of pixel i and it takes value within a finite set.
Denote ∂_i and $|\partial_i|$ as the first order neighborhood of the pixel i and the number of
pixels inside this neighborhood (pixel i itself is also a member of this neighbor). The
RT is defined as:

$$T(X) = \{y_i : y_i \equiv \frac{\sum_{k \in \partial_i \cap S} x_k}{|\partial_i \cap S|}, i \in S\}. \quad 2.1$$

20      $T(X)$ is a new image with the same pixel location and its intensity value
of each voxel is the average intensity of those of pixels in its neighborhood. The RT
is a linear transformation and can be calculated locally. This makes it possible for a
fast parallel implementation.

The estimation of the bias field is to apply RT iteratively to the MR

25   image X. When the condition $\max_{i \in S} |T^{(n)}(X)_i - T^{(n+1)}(X)_i| \leq t$ is satisfied, $T^{(n)}(X)$ is the
estimation of the bias field, where n is the number of iteration and t is a pre-set
threshold. For example, we can set t as the average intensity of the image X dividing
by 3000.

The bias field is often modeled as the following classical way:

$$Y = X \cdot f + n \qquad 2.2$$

where Y is the obtained MR image, X is the ideal image without inhomogeneity, f is the bias field, and n is the noise. Ignoring the noise component, the image data is the

5   multiplication of the ideal image and the bias field. Following this model, the correction procedure can be performed by dividing the image data by the estimated inhomogeneity bias field. However, in the RT model, the RT is a linear transformation rather than a multiplication transformation. Therefore, the following model is more accurate for RT method:

10                                $$Y = X + f + n \qquad 2.3$$

Where Y, X, n, and f were defined above. For correction algorithms ignoring the noise, we induce the following model:

$$X = Y + \alpha \cdot (\hat{f} - M_0) \qquad 2.4$$

where $\alpha(\hat{f} - M_0)$ is a linear transform applied on the estimated bias

15   field $\hat{f}$, α is a scaling factor and M_0 is an image calculated from X. This model assumes that all pixels represent a common tissue type. In practical situations, however, this is not the case. Hence, a correction model is applied in a flexible way to ensure that the assumption is satisfied to the greatest degree possible. For example, the image can be processed on a row by row or column by column basis.

20   Alternatively, image segmentation can be performed initially and regions of substantially common tissue types can be delineated and separately processed by applying the model to each region. The determination of α and M_0 should also be adaptive to the practical situation. For example, we can set $\alpha = -1$ and compute M_0 as the average intensity of the image.

25   Image Segmentation

A difficulty encountered in imaging is that several of the relevant anatomical structures have similar intensity values on the CT image. This can make it difficult to distinguish the various structures which overlap or are interrelated. To address this problem, a two-level image segmentation process can be employed. The

two-level segmentation process involves low-level processing of the voxels in the region of interest followed by high-level organ extraction. During the low-level processing, the voxels of the 3D dataset are clustered into groups based on an intensity feature of the voxels, which can be measured by an associated local intensity

5   value vector. This can be determined using a modified self-adaptive on-line vector quantization algorithm, such as is described in the article "A self-adaptive on-line vector quantization algorithm for MRI segmentation," by Chen et al. in the proceedings of The 7th Scientific Meeting of ISMRM, May 1999, Philadelphia, which is hereby incorporated by reference. In the low-level classification, each voxel is

10 associated with a local vector which is defined in 3D space. From the local vectors, a feature vector series can be derived using a components analysis which is well known in the art. The feature vectors are then clustered using a self-adaptive on-line vector quantization algorithm. The voxels are then grouped according to the classification of their feature vectors and are assigned an integer value representing this classification.

15   After the low-level processing is complete, the high level organ extraction processing can follow. Initially, a user locates a seed, or starting point, within regions representative of soft tissue, bone and air spaces. The system then applies a region growing algorithm starting from the seed points to extract the anatomical features of the region.

20   Bone structure, which presents different contrast compared to the surrounding tissues is fairly easy to automatically segment. However, certain structures may require additional user input to fully delineate these structures. For example, the soft tissue of the inner ear presents a similar intensity value on CT images as compared to the surrounding soft tissue. Thus, to insure proper extraction

25 of such features, it may be desirable for the user to manually delineate the outline of the structure by manually tracing the contour on one or more of the image slices.

        While the above described two level image segmentation is preferred, any method which provides accurate delineation of the neighboring structures in a region of interest can be used in the practice of the present treatment planning

30 method. One such technique is described in the article "On segmentation of colon

lumen for virtual colonoscopy" by Liang et al., Proceedings of SPIE Medical
Imaging, pp 270-278, Feb. 1999, San Diego.

Once image segmentation is performed, 3D image generation can be
performed for each of the segmented objects using a number of known techniques,

5   such as the Marching Cubes algorithm, which reconstructs the outer polygonal
surface. However, because of the complexity of many anatomical structures,
interactive rendering of all polygons in the display for each change to a portion of the
display is processor intense and unduly costly. As more colors and surfaces are
delineated in the displayed image, this burden increases. To minimize the processing

10   overhead, the volume image dataset can be stored in a partitioned data structure, such
as a binary space-partitioning (BSP) tree, in which the large dataset is parsed into
relatively small portions which are stored in leaf nodes of the data structure. By
identifying which leaf nodes are effected by any given operation, and only performing
operations, such as Constructive Solid Geometry (CSG) operations, on the effected

15   leaf nodes, the processing burden for interactive operations can be significantly
reduced. As will be set forth in more detail below, the processing burden can be
further reduced by use of a level of detail (LOD) rendering mode and/or a wavelet
transformation to reduce the data volume.

As noted above, when a large dataset is involved, it may be required,

20   or at least desirable, to reduce the size of the dataset to speed up processing and
reduce processing cost. Noting that the tree structure can be preserved within a range
of scales, the large volume can be shrunk to a smaller scale space for structure
analysis.

A shrinking method based on multiresolution analysis theory can be

25   used. The input data is the stack of binary images of the same size which can be
obtained from the segmentation results of the CT or MRI scan. The x-direction is
taken along the slice image width, the y-direction is along the slice image height, and
the z-direction is along the direction of slice by slice. The foreground voxels in the
tree volume are set to value of 128 (maximum) and the background voxels are set to

30   value 0 (minimum). A Daubechies' bi-orthogonal wavelet transform with all rational
coefficients can be employed. This one-dimensional (1D) discrete wavelet

22

transformation (DWT) is first applied along to the x-direction row by row. From application of the DWT only the lower frequency components are retained and packed. The computation is preferably implemented in floating points. Noting that the DWT is applied to the binary signal, there are two kinds of nonzero coefficients

5   which result in the lower frequency component. The first is of value 128 and this kind of coefficient is located in the interior of the volume. The second is of a value not equal to 128 and these coefficients locate the boundary of the volume.

The coefficients of the second kind are compared against a predetermined threshold value. If the absolute value of the coefficients is larger than

10   a pre-set threshold **T1**, the value of the coefficient is set to 128; otherwise, it is set to 0. This results in a stack of binary images with a row size of half of the original dataset. The same DWT is then applied to the resulting dataset along the y-direction column by column, where the similar thresholding is employed to the lower frequency components. The result is again a stack of binary images, but now with both half row

15   and column size as compared to the original dataset. Finally, the DWT is applied to the last result along the z-direction and the lower frequency components are retained. This step completes the first level decomposition.

The resulting dataset of the first level decomposition is of half size in all three directions as compared to the original dataset. If the shrinking procedure

20   stops at this level, the finial thresholding is applied. It revalues those coefficients of nonzero and non-128 value. If the absolute value of this kind of coefficient is larger than a pre-set threshold **T2**, it will be revalued as 128; otherwise, it is revalued as 0. If further shrinking is needed, the same thresholding algorithm is applied with the threshold **T1**. Further shrinking proceeds as previously described, but is applied to

25   the dataset shrunk at the last previous level. The decomposition procedure can be recursively applied until the resulting volume meets the desired reduced data volume. In the case where the slice images are of 512X512 pixel size, the maximum decomposition level is usually three, resulting in a 64x64 reduced pixel size.

The volume is isotropically shrank in all directions with the presented

30   method. The two pre-set thresholds, **T1** and **T2**, are used to control the degree of shrinking. If the volume is significantly over shrunk, connectivity may be lost in the

reduced volume. If it is over shrunk to a lesser degree, two separate branches may merge into one branch in the reduced volume dataset. The larger the two threshold values, the thinner the reduced volume is. The range of those two thresholds is [0, r x 128], where 0<r<1. Preferably, the range for virtual endoscopy is r∈ (0.08, 0.28) for

5   **T1** and r∈ (0.7, 0.98) for **T2**. The exact determination is dependant on the feature size of the particular application and is selected to achieve reduction while retaining the fidelity of the structure information in the shrunk volume..

The flexible image registration techniques and spatial inhomogeneity corrections are applicable to surgical planning processes. For example, in the case of

10   angioplasty, the surgeon inserts a catheter into an occluded artery and inflates a balloon at the end of the catheter to force the occluded artery open and to expand a stent which maintains the opening. While this has become a common procedure, it is not without risk. For example, the arterial occlusion is generally related to a build up of plaque and fatty deposits on the arterial wall. If a portion of these deposits are

15   dislodged during the angioplasty process or if the region of plaque ruptures, there is a risk of stroke and other complications. Using the present method of treatment planning, the artery can be imaged and, through image segmentation, the quantity and nature of the plaque deposits can be determined. The severity of the occlusion can be viewed by the surgeon who can navigate in the 3D image within the artery. A virtual

20   intervention can then be performed, i.e., placing a virtual catheter within the arterial volume and expanding a virtual stent, and the results observed. If problems are observed, such as a high risk of rupture, the user can then alter the course of treatment to minimize the risk. The virtual catheter and stent require a dynamic model that conforms to the contours of the interior surface of the arterial wall. Such a model is

25   analogous to the force field model previously used in guiding a virtual camera along a fly path in performing virtual colonoscopy.

Known volume rendering techniques use one or more defined transfer functions to map different ranges of sample values of the original volume data to different colors, opacities and other displayable parameters for navigation and

30   viewing. During navigation, the selected transfer function generally assigns maximum opacity to the wall of the object being viewed. However, once a suspicious

area is detected during virtual examination, a user, such as a physician, can interactively change the transfer function assigned during the volume rendering procedure such that the outer surface being viewed becomes substantially transparent, allowing the interior structure of the region to be viewed. Using a number of

5   predetermined transfer functions, the suspicious area can be viewed at a number of different depths, with varying degrees of opacity assigned throughout the process. In addition, the shape of the region and texture of the region undergoing virtual examination can be analyzed to determine the nature of the region, such as a likelihood of cancerous tissue residing in a region being biopsied.

10   Although the present invention has been described in connection with specific exemplary embodiments, it should be understood that various changes, substitutions and alterations can be made to the disclosed embodiments without departing from the spirit and scope of the invention as set forth in the appended claims.

CLAIMS

1.   A computer based method of visualizing a region using multiple image data sets comprising:

acquiring first volumetric image data of a region;

5   acquiring at least second volumetric image data of the region;

determining structural features of the region using the first volumetric image data

determining at least one control point in the region using at least one structural feature in the first volumetric image data;

10   identifying the at least one control point in the region in the at least second image data of the region;

registering the first image data and the at least second image data using said at least one control point; and

fusing the registered first image data and at least second image data into a

15   common display data set.

2.   The method of visualizing a region using multiple image data sets of claim 1, wherein the region includes a branched structure having a common section and at least two branches extending from the common section forming a bifurcation region and wherein said control point is the bifurcation point of the branched structure.

20   3.   The method of visualizing a region using multiple image data sets of claim 2, wherein the bifurcation point is determined as the center of an imaginary maximal diameter sphere which is fit within the bifurcation region.

4.   The method of visualizing a region using multiple image data sets of claim 3, wherein the branched structure in a blood vessel.

25   5.   The method of visualizing a region using multiple image data sets of claim 1, wherein the at least second volumetric image data is acquired using a mode which is different from a mode used to acquire the first volumetric image data.

6.   The method of visualizing a region using multiple image data sets of claim 5,
wherein the mode used to acquire the at least second image data is selected to provide
complimentary imaging characteristics to the mode used to acquire the first image
data.

5   7.   The method of visualizing a region using multiple image data sets of claim 1
wherein the second volumetric image data is acquired at a substantially different time
from said first volumetric image data.

8.   The method of visualizing a region using multiple image data sets of claim 1,
wherein the second volumetric image data is acquired with the patient in an
10   orientation which is different than an orientation used during acquisition of the first
volumetric image data.

9.   A method of visualizing and analyzing a region of artery comprising:
       acquiring first volumetric image data of a region of artery using a first
acquisition mode;
15   acquiring at least second volumetric image data of the region of artery using a
second acquisition mode, said second acquisition mode being different than the first
acquisition mode;
       determining structural features of the artery using the first volumetric image
data;
20   determining a bifurcation point in the artery using the first volumetric image
data;
       defining a coordinate system with the bifurcation point as the origin;
       identifying the bifurcation point in the artery in the at least second image data
of the region and applying the defined coordinate system to the at least second
25   volumetric image data;
       registering the first volumetric image data and the at least second volumetric
image data using the bifurcation point and coordinate system; and
       fusing the registered first volumetric image data and at least volumetric second
image data into a common display data set.

27

10.   The method of visualizing and analyzing a region of artery of claim 9, wherein the structural features include at least one region of stenosis resulting at least in part from a plaque deposit, and wherein the method further comprises the steps:

identifying the location of the at least one region of stenosis in the first

5   volumetric image data;

using the location from the first volumetric image data, determining the location of the stenosis in the at least second volumetric image data.

11.   The method of visualizing and analyzing a region of artery of claim 9, wherein the step of identifying the location of the at least one region of stenosis includes

10   measuring the distance along at least one axis of the coordinate system from the bifurcation point to a point in the region of stenosis

12.   The method of visualizing and analyzing a region of artery of claim 10, wherein the at least second acquisition mode is selected to delineate fatty components of the plaque deposits.

15   13.   The method of visualizing and analyzing a region of artery of claim 10, wherein the at least second acquisition mode is selected to delineate calcification components of the plaque deposits.

14.   The method of visualizing and analyzing a region of artery of claim 10, wherein the at least second acquisition mode includes second and third acquisition

20   modes, at least one of the second and third acquisition modes being selected to delineate fatty components of plaque deposits and at least one of the second and third acquisition modes being selected to delineate calcification components of plaque deposits.

15.   The method of visualizing and analyzing a region of artery of claim 14,

25   wherein the first acquisition mode is Magnetic Resonance Angiograpy.

16.   The method of visualizing and analyzing a region of artery of claim 14, wherein the first acquisition mode is ultrasound imaging.

17.   The method of visualizing and analyzing a region of artery of claim 14, wherein the second acquisition mode is T_1-weighted MR imaging.

18.   The method of visualizing and analyzing a region of artery of claim 14, wherein the second acquisition mode is T_2-weighted MR imaging.

5   19.   The method of visualizing and analyzing a region of artery of claim 14, wherein the first acquisition mode is time-of-flight Magnetic Resonance Angiograpy, the second acquisition mode is T1-weighted MRI imaging, and the third acquisition mode is Computed Tomography imaging.

20.   The method of visualizing and analyzing a region of artery of claim 9, further
10   comprising analyzing a plaque deposit identified in the fused image data.

21.   The method of visualizing and analyzing a region of artery of claim 20, wherein the analyzing step includes determining the composition of the plaque deposit.

22.   The method of visualizing and analyzing a region of artery of claim 21,
15   wherein the analyzing step includes determining the volume and position of fatty components in the plaque deposit.

23.   The method of visualizing and analyzing a region of artery of claim 21, wherein the analyzing step includes determining the volume and position of calcification components in the plaque deposit.

20   24.   The method of visualizing and analyzing a region of artery of claim 21, wherein the analyzing step includes determining the volume and position of blood components in the plaque deposit.

25.   The method of visualizing and analyzing a region of artery of claim 20, wherein the analyzing step further comprises assessing the risk of rupture of the
25   plaque deposit.

26.　　A method for correcting spatial inhomogeneity in magnetic resonance imaging
data comprising:

　　　　acquiring MRI image data;

　　　　estimating a bias field associated with the MRI image data; and

5　　　　applying the bias field to the MRI image data to provide corrected MRI image
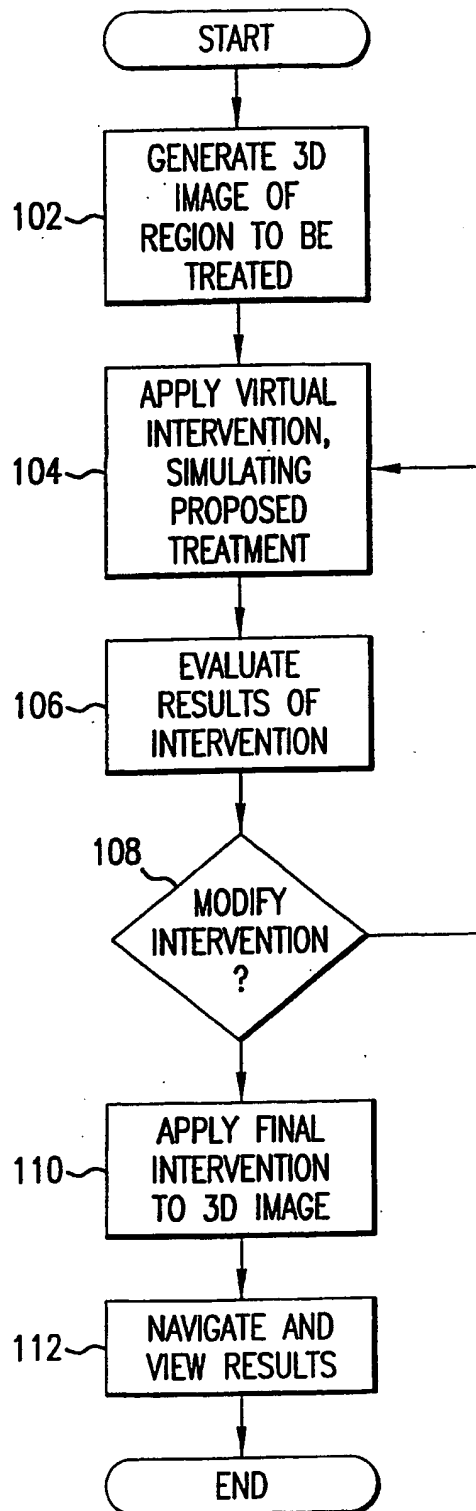data.

```
                    ┌─────────────┐
                    │    START    │
                    └─────────────┘
                           │
                           ▼
                   ┌───────────────┐
                   │  GENERATE 3D  │
                   │   IMAGE OF    │
           102 ─── │ REGION TO BE  │
                   │    TREATED    │
                   └───────────────┘
                           │
                           ▼
                   ┌───────────────┐
                   │ APPLY VIRTUAL │
                   │ INTERVENTION, │◄──────────┐
           104 ─── │  SIMULATING   │           │
                   │   PROPOSED    │           │
                   │   TREATMENT   │           │
                   └───────────────┘           │
                           │                   │
                           ▼                   │
                   ┌───────────────┐           │
                   │   EVALUATE    │           │
           106 ─── │  RESULTS OF   │           │
                   │ INTERVENTION  │           │
                   └───────────────┘           │
                           │                   │
                           ▼                   │
                108      �◊              │
                       ╱  MODIFY  ╲────────────┘
                       ╲INTERVENTION╱
                        ╲    ?    ╱
                           │
                           ▼
                   ┌───────────────┐
                   │  APPLY FINAL  │
           110 ─── │ INTERVENTION  │
                   │  TO 3D IMAGE  │
                   └───────────────┘
                           │
                           ▼
                   ┌───────────────┐
           112 ─── │ NAVIGATE AND  │
                   │ VIEW RESULTS  │
                   └───────────────┘
                           │
                           ▼
                    ┌─────────────┐
                    │     END     │
                    └─────────────┘
```

FIG.1

FIG.2

FIG. 3

305　ACQUIRE FIRST IMAGE DATA

310　ACQUIRE ADDITIONAL IMAGE DATA

315　DETERMINE STRUCTURAL CHARACTERISTICS OF REGION

320　ESTABLISH CONTROL POINTS BASED ON IDENTIFIABLE STRUCTURAL CHARACTERISTICS

325　DETECT SUSPECT REGION USING ONE SET OF IMAGE DATA

330　REGISTER IMAGE DATA USING CONTROL POINTS

335　DETERMINE SUSPECT REGION IN SECOND IMAGE DATA BASED ON CONTROL POINT AND FIRST IMAGE DATA

340　SEGMENT IMAGE DATA AND ANALYZE

345　FUSE AND DISPLAY IMAGE DATA

FIG. 4
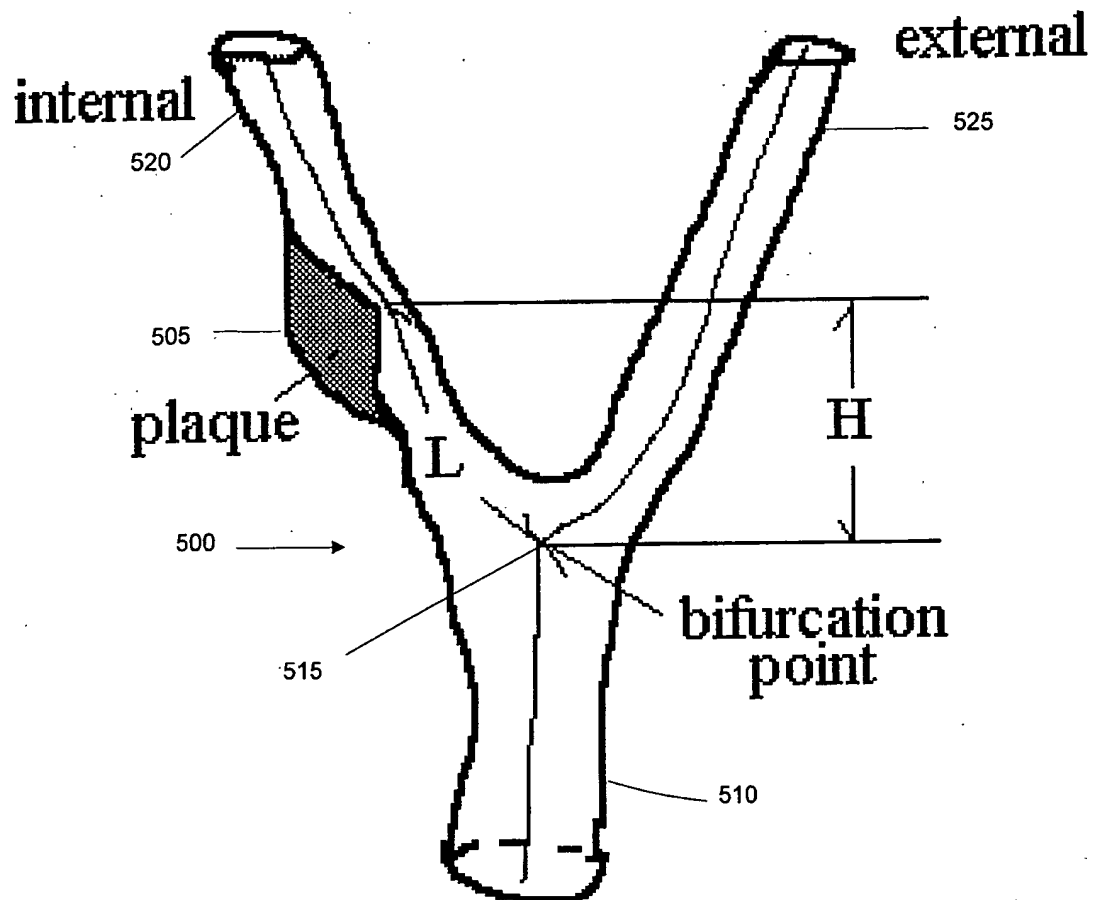
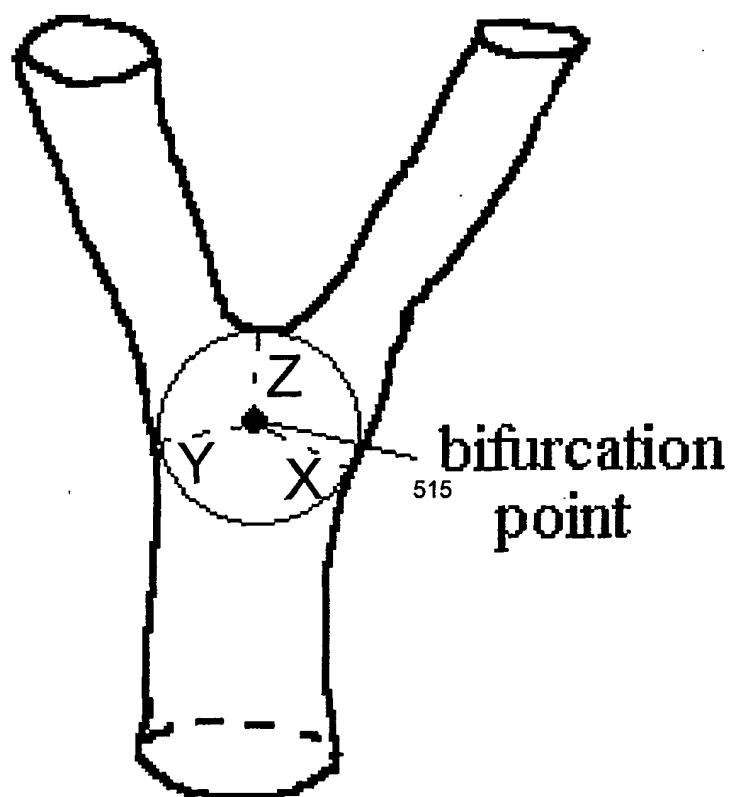

NASCET :

$$\frac{B-A}{B} \times 100\%$$

A : stenosis
B : normal

FIG. 5

FIG. 6

bifurcation point

FIG. 7A

FIG. 7B

FIG. 8

805 — ACQUIRE IMAGE OF REGION INCLUDING ARTERIAL STRUCTURE

810 — IDENTIFY ARTERIAL WALL AND LUMEN

815 — LOCATE CONTROL POINT

820 — LOCATE SUSPECT REGIONS WITH RESPECT TO CONTROL POINT

825 — ACQUIRE IMAGE DATA FOR FATTY COMPONENTS OF PLAQUE

830 — LOCATE SUSPECT REGIONS IN T1-WEIGHTED MRI USING CONTROL POINT AND POSITION FROM FIRST IMAGE DATA

835 — PERFORM SEGMENTATION OF SUSPECT REGIONS

840 — ACQUIRE IMAGE DATA FOR CALCIFICATION COMPONENTS

845 — IDENTIFY CONTROL POINT AND POSITIONS OF SUSPECT REGIONS IN IMAGE DATA

850 — PERFORM SEGMENTATION OF SUSPECT REGIONS

855 — FUSE IMAGES

860 — ANALYZE SUSPECT REGIONS

8/10

FIG. 9

```
┌─────────────────┐
│  ACQUIRE MRI    │──── 905
│  IMAGE DATA     │
└─────────────────┘
         │
         ▼
┌─────────────────┐
│    ESTIMATE     │──── 910
│   BIAS FIELD    │
└─────────────────┘
         │
         ▼
┌─────────────────┐
│  CORRECT MRI    │
│  DATA USING     │──── 915
│   ESTIMATED     │
│   BIAS FIELD    │
└─────────────────┘
```

FIG. 10